

ADM-Aeolus vertical sampling scenarios

Gert-Jan Marseille¹, Ad Stoffelen¹, Jos de Kloe¹, Karim Houchi¹, Heiner Körnich², H. Schyberg³, Anne Grete Straume⁴, Olivier LeRille⁴

¹ Royal Dutch Meteorological Institute (KNMI), P.O. Box 201, NL 3730 AE, De Bilt, The Netherlands
e-mail: Gert-Jan.Marseille@knmi.nl

² Meteorology Department Stockholm University (MISU), Svante Arrhenius väg 12, Stockholm, Sweden

³ Norwegian Meteorological Institute, PO Box 43 Blindern, Oslo, Norway

⁴ ESA/ESTEC, Postbus 299, NL 2200 AG, Noordwijk, The Netherlands

ABSTRACT

The Atmospheric Dynamics Mission ADM-Aeolus is scheduled for launch in April 2011. ADM-Aeolus is a polar orbiting satellite at 400 km altitude carrying a Doppler wind lidar (DWL) to measure wind profiles from the surface up to 30 kilometres altitude. It is the first observing system to provide a global 3D coverage of atmospheric winds and as such fills in the major deficiency of the current global observing system as recognized by the WMO.

In preparation for launch we aim to optimize the vertical sampling of ADM by defining strategies for the distribution of the 24 vertical bins. The flexibility to change the vertical sampling scenario with a maximum of 8 times per orbit opens the possibility of targeted strategies for the various geographic regions.

The definition of a high-resolution database of atmospheric dynamics and optical properties based on ECMWF model parameters and CALIPSO satellite data is discussed. The database serves as input to select vertical sampling scenarios that maximize the information content of retrieved winds taking into account the atmosphere heterogeneity.

1. INTRODUCTION

ADM-Aeolus carries a single fixed beam direct-detection high spectral-resolution DWL. The laser is operated at 355 nm with a 100 Hz pulse repetition frequency and pointed towards the atmosphere with a 35 degrees incidence angle. ADM thus measures a single wind component, along the laser beam line-of-sight (LOS), and not the complete wind vector. The DWL is operated in so-called burst mode, meaning that the laser is turned on for 7 seconds (50 km along track) and turned off for 21 seconds to save energy. As a result, a wind profile is obtained every 200 km along track, see Fig. 1.

ADM-Aeolus is operated in the UV part of the electromagnetic spectrum at 355nm meaning that backscattered light originates from both molecules and particles (aerosols, cloud droplets). Backscattered light is detected by two independent spectrometers. A dual channel Fabry-Perot spectrometer measures both sides of the broad Rayleigh-Brillouin (molecular) spectral peak, and a high resolution Fizeau spectrometer measures the location of the narrow Mie (particle) peak [1]. The vertical resolution of both spectrometers is limited to 24 bins. There is some flexibility in the positioning of these bins. The minimum bin size is 250 m, the maximum bin size is 2000 m. All values in between that are multiples of 250m are allowed.

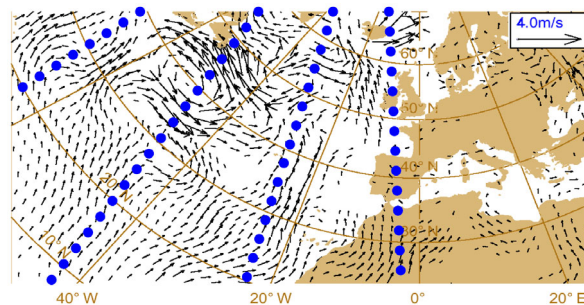


Figure 1. ADM-Aeolus horizontal sampling of relevant wind structure over the Northern Atlantic. Blue dots show 4 orbits with wind profile locations that are separated by 200 km along track.

In flight the vertical sampling scenario may be changed with a maximum of 8 times per orbit. This opens the possibility of targeted strategies for the various geographic regions, e.g. clouds are rarely found above 10 km in the polar regions, but frequently near 15 km in the Tropics. Mie bins positioned at 15 km are therefore not very effective in polar regions, but can be in the Tropics. Other considerations in designing vertical sampling scenarios are i) Signal-to-noise ratio (SNR), i.e. the bin size must be sufficiently large to gather signal with a SNR sufficient to meet the wind quality mission requirements, ii) some of the Mie channel bins must be "sacrificed" to guarantee ground returns for zero wind calibration (ZWC) [2], iii) in heterogeneous atmospheric scenes such as the PBL and jet streams, Mie oversampling is potentially useful to obtain representative winds. Every 3 weeks a new table of scenarios is uploaded to the instrument.

Heterogeneous atmospheric scenes with large dynamical and optical variability are the most challenging for wind retrieval. In the following sections the spatial distributions of the occurrence of large wind-shear events and optical variability are presented as a function of season based on ECMWF model winds and CALIPSO backscatter data.

2. ATMOSPHERE DYNAMICS

Four three-month periods, covering all seasons, of archived ECMWF global model wind field analyses have been used to generate statistics of wind-shear and vertical wind velocity. Model analyses are available at 00, 06, 12 and 18 UTC. The model resolution is T799L91, i.e. about 25 km horizontal resolution and 91 vertical levels that extend from the surface up to 0.01 hPa, i.e. about 85 km.

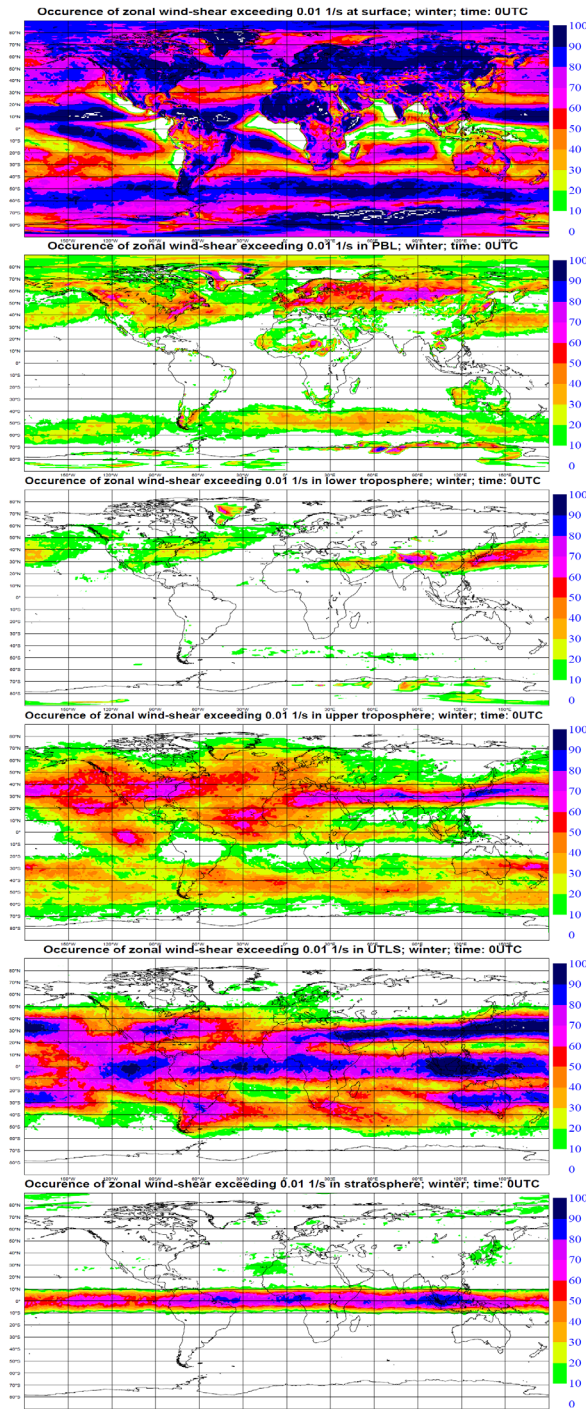


Figure 2. Occurrence of large shear (exceeding 0.01 s^{-1}) for the 00 UTC ECMWF model zonal wind component for the 3-month period December-January-February 2006/7. From top to bottom: surface, PBL, lower troposphere, upper troposphere, UTLS and stratosphere. These height layers are defined in the text.

Figure 2 shows statistics of the occurrence of large vertical wind-shear, exceeding a threshold value of 0.01 s^{-1} , i.e. 10 ms^{-1} per km, for the zonal wind component in the winter (DJF) period for various height layers. The height layers are defined as follows; *Surface*: the first 250 m above the earth surface, *PBL*: the range from 250 m above the earth surface until 3 km above mean sea level (MSL), *Lower Troposphere*: the

range from 3-7 km above MSL, *Upper Troposphere*: the range from 7-15 km above MSL, covering the extra-tropical jets, *Upper Troposphere-Lower Stratosphere (UTLS)*: the range from 15-22 km above MSL, covering the tropical jet, *Stratosphere*: the range from 22-30 km above MSL. A consequence of this choice for the height layer definition is the presence of data void areas in the PBL for mountainous regions with orography exceeding 3 km above MSL. The same is true for the lower troposphere plot in mountainous regions exceed 7 km above MSL.

The wind-shear of the zonal wind component exceeds the threshold value of 0.01 s^{-1} frequently near the surface as shown in the top panel of Figure 2. This is the case in particular over the continents most probably due to orography but also over the oceans, in particular in the Southern Hemisphere and in the tropical trades, away from the mainland. In the PBL the occurrence of large wind-shear is much less with maximum values over the Northern Hemisphere (NH) continent. The least shear is found in the lower troposphere between 3 and 7 km above MSL with maximum values found in the NH over the Pacific and over China. In the upper troposphere substantial large shear events are observed covering the full globe except the Polar regions. Maximum occurrence is found near the NH jet stream. A large occurrence of large shear events is also found in the UTLS but limited to the Tropics and sub-Tropics. In the stratosphere the occurrence of large shear events is mainly limited to a small area around the equator between 10N and 10S.

Comparing to 6, 12 and 18 UTC statistics (not shown, but found in [3]) a diurnal cycle of the occurrence of large shear events is observed mainly near the surface and in the PBL. The diurnal cycle is most prominent over the continents with maximum shear values found between local midnight and dawn and substantially less at local daytime. This can be explained by well-developing nocturnal boundary layers during the night accompanied with an increasing wind-shear on top of the inversion. After sunrise, the stabilized PBL starts to breakdown due to turbulence, thus removing the inversion and accompanied wind-shear.

Statistics of other seasons show similar characteristics however with a shift of the occurrence of large shear events from the Northern to the Southern Hemisphere, i.e. following the hemisphere winter season [3]. The meridional wind is of less importance because of the pointing geometry of ADM that is close to zonal for most part of the orbit [4]. Also the occurrence of large shear events for the meridional wind is substantially less than for the zonal wind [3].

3. ATMOSPHERE OPTICS

The successful CALIPSO satellite offers a unique dataset of atmospheric (attenuated) backscatter at 532 nm laser wavelength covering the full globe and all seasons over more than 3 years now. A scheme has been developed to retrieve aerosol and cloud optical properties from CALIPSO data at 355 nm wavelength at high resolution, i.e. 3.5 km along orbit and 125 m in the vertical. The first step is to reduce the raw CALIPSO level-1 attenuated backscatter data to this resolution. In the second step all profiles are proc-

essed individually. The equation for attenuated backscatter is

$$\beta^{532}(z) = [\beta_c^{532}(z) + \beta_a^{532}(z) + \beta_m^{532}(z)] \cdot [\tau_c^{532}(z) \tau_a^{532}(z) \tau_m^{532}(z) \tau_{O_3}^{532}(z)]^p \quad (1)$$

with β the measured attenuated backscatter ($\text{m}^{-1}\text{sr}^{-1}$), β backscatter ($\text{m}^{-1}\text{sr}^{-1}$) and τ one-way atmospheric transmission defined through

$$\tau_i^{532}(z) = \exp \left[- \int_z^{h_{\text{sat}}} \alpha_i^{532}(z') dz' \right] \quad (2)$$

with α extinction (m^{-1}). The exponents refer to the wavelength in (nm). The indices {c,a,m} refer to clouds, aerosols and molecules respectively, τ_{O_3} is transmission through ozone. Cloud and aerosol backscatter and extinction are related through the so-called lidar ratio S :

$$\alpha_i^{532}(z) = S_i^{532}(z) \beta_i^{532}(z) \quad i = \{c, a\} \quad (3)$$

The lidar ratio is a function of the particle properties that are generally unknown. Molecular backscatter and transmission are obtained from given atmospheric temperature and pressure. Ozone transmission is obtained from the ancillary CALIPSO data.

In a first step clouds and aerosols are discriminated based on signal thresholding. For isolated clouds, the 2-way cloud transmission is obtained from the ratio of the measured signal below the cloud and the expected signal for a cloud-free atmosphere. The cloud lidar ratio and cloud backscatter then follow from fitting Eq. (1) to the measured data inside the cloud layer iteratively, ignoring the presence of aerosols. For non-isolated clouds, default values for the cloud lidar ratio are used based on the water phase.

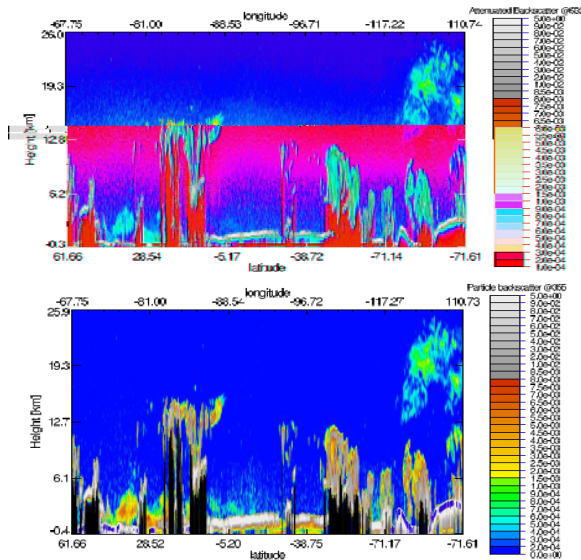


Figure 3. CALIPSO level-1 attenuated backscatter at 532 nm at 3.5 km horizontal and 125 m vertical resolution (top) and retrieved particle backscatter at 355 nm (bottom). The measurement date is 4 August 2007. Black spots in the bottom figure denote regions where no backscatter could be retrieved due to low SNR in the level-1 data.

After having determined the cloud optical properties 2 unknowns are left in Eq. (1), i.e. aerosol backscatter and extinction that are related through Eq. (3). Without a priori knowledge a value of 35 (sr) is used for the aerosol lidar ratio that is typical for background aerosol. Eq. (1) is then solved and a validity check applied to eventually adapt the value of the aerosol lidar ratio.

Conversion from 532 nm to 355 nm is then performed through the angstrom exponent x [5] and the lidar ratio at 355 that is assumed identical to the value at 532 nm:

$$\alpha_i^{355}(z) = \alpha_i^{532}(z) \left(\frac{532}{355} \right)^x \quad i = \{c, a\} \quad (4)$$

$$\beta_i^{355}(z) = \alpha_i^{355}(z) / S_i^{355}(z) \quad i = \{c, a\} \quad (5)$$

Figure 3 shows an example of retrieved particle backscatter from CALIPSO level-1 raw attenuated backscatter data for a nighttime orbit, clearly showing polar stratospheric clouds (PSC) over the South Pole region.

4. ECMWF-CALIPSO COLLOCATION

To determine the occurrence of heterogeneous scenes of both large wind-shear and optical variability the atmospheric dynamics from ECMWF along the CALIPSO orbit was combined with CALIPSO retrieved backscatter. This collocated dataset was searched for events of combined large wind-shear exceeding 0.01 s^{-1} and a discontinuity in the particle backscatter.

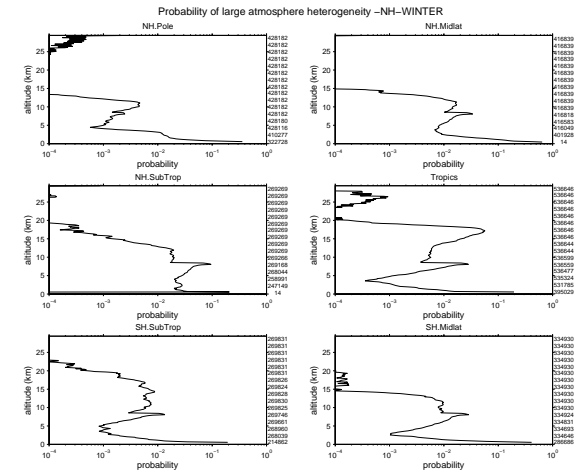


Figure 4. Probability (in log-scale) of the occurrence of strong wind-shear ($>0.01 \text{ s}^{-1}$) in combination with large backscatter variability (more than one order) as a function of climate zone for January 2007.

Figure 4 shows the occurrence rate of heterogeneous scenes in January 2007 for 6 climate zones: NH polar region ($> 70^\circ\text{N}$), NH mid-latitude region (40°N - 70°N), NH subtropics (20°N - 40°N), Tropics (20°S - 20°N), SH subtropics (20°S - 40°S) and SH mid-latitude region (40°S - 70°S). No statistics are available for the SH polar region, because it is lit by the sun in August, so no nighttime orbit CALIPSO data are available. The probability of an extreme event is generally small and below 5% at each altitude. Only in the PBL the probability exceeds 10% with a maximum value of about 60% near the

surface in the Northern Hemisphere mid-latitudes. At higher altitudes extreme events are related to clouds. The Northern Hemisphere subtropics shows a maximum of about 10% at the jet stream level near 8 kilometer altitude. The maximum occurrence in the tropics of ~6% is found at 17 km altitude.

Similar statistics for the other seasons are found in [3] and show most extreme events in the winter periods. PSCs in the Southern Hemisphere (SH) polar region in August yield substantially more heterogeneous scenes above 15 km in the NH-summer (i.e. SH-winter) statistics.

The small amount of extreme events in the statistics of Figure 4 is explained by the relative smooth fields of global models like ECMWF, i.e. ECMWF contains too little variability on the smaller scales below 500 km, with about an order of magnitude too small energy content at 100 km wavelength. The lack of variance in the ECMWF wind and shear is most likely related to too high levels of dissipation on the small scales in the numerical closure scheme of the advection equations. An algorithm has been devised and tested to add small-scale variance to the ECMWF model to bring the shear and wind variability in line with high-resolution radiosonde measurements [6]. With this, we can simulate scenes with realistic optical and dynamical variability by combining our CALIPSO retrievals and collocated post-processed ECMWF data. The occurrence rate of atmospheric scenes with strong dynamical and optical variability is then increased by an order of magnitude to about 10%. Maximum occurrence rates up to 35% were found near the tropopause for all climate regions [3].

5. CONCLUSIONS

CALIPSO retrieved optical properties have been collocated with ECMWF model winds to provide statistics of the occurrence of heterogeneous atmospheric scenes as a function of season and geographic location.

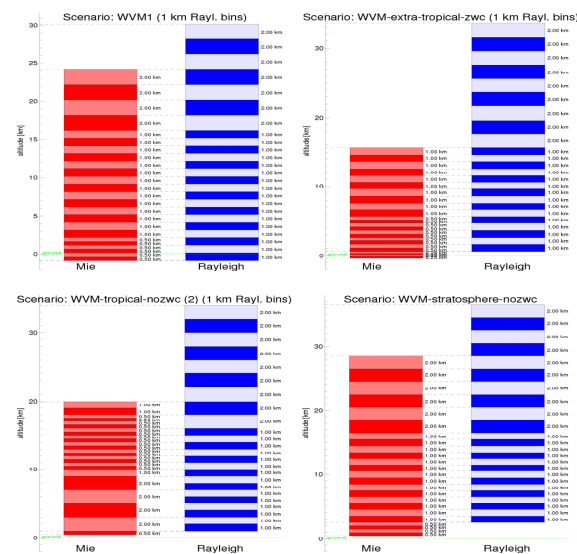


Figure 5. Optional ADM vertical sampling scenarios: default (top left), extra-tropical (top right), tropical (lower left) and stratosphere (lower right). The positioning of the Mie/Rayleigh channel bins is in red/blue.

Based on the generated statistics a first selection of vertical sampling strategies for ADM was made, see Figure 5. The minimum size for Rayleigh bins is 1 km to yield sufficient SNR to meet the mission wind quality requirement. The default scenario enables ZWC with the Mie channel and has a maximum number of overlapping Mie and Rayleigh bins. Virtually all particles are captured with a Mie channel up to 24 km. The maximum altitude of the Mie channel in the extra-tropical/tropical scenarios is 15/20 km. The latter has increased resolution near the tropopause to enable wind retrieval in heterogeneous atmospheres. The stratospheric scenario has maximum Mie/Rayleigh coverage in the stratosphere, meets the mission wind requirement but has no ZWC capability. The information content of non-overlapping bins has not been studied so far.

The generated collocated ECMWF-CALIPSO database is used in a next stage to further assess these sampling scenarios through i) application of the lidar performance analysis tool (LIPAS) [7], ii) a new developed analytical tool based on the theoretical analysis equations and iii) assimilation ensemble experiments with the ECMWF model [8].

REFERENCES

- [1] Stoffelen A., J. Pailleux, E. Källén, J.M. Vaughan, L. Isaksen, P. Flamant, W. Wergen, E. Andersson, H. Schyberg, A. Culoma, M. Meynart, M. Endemann, P. Ingmann, 2005: The Atmospheric dynamics mission for global wind measurement, Bull. Am. Meteorol. Soc., **86**, pp. 73-87.
- [2] Kloe de J., A. Stoffelen, G.J. Marseille, D. Tan, L. Isaksen, C. Desportes, C. Payan, A. Dabas, D. Huber, O. Reitebuch, P. Flamant, H. Nett, Ol. Le Rille' A.G. Straume, 2009: ADM-Aeolus Ocean Surface Calibration and Level-2B Wind-Retrieval Processing, this proceedings.
- [3] Stoffelen, A., H. Kornich, G.J. Marseille, K. Houchi, J. de Kloe, 2009: Assessment of Optical and Dynamical Atmospheric Heterogeneity, ESA Technical Note AE-TN-KNMI-VAMP-002_v7, available through ESA-ESTEC.
- [4] Straume, A.G. et al., this proceedings.
- [5] Mattis, I., Ansmann, A., Müller, D., Wandinger, U. and Althausen, D., 2004: Multiyear aerosol observations with dual-wavelength Raman lidar in the framework of EARLINET, J. Geoph. Res., **109**, D13203, doi:10.1029/2004JD004600
- [6] Houchi, K., A. Stoffelen, G.J. Marseille, J. de Kloe, 2009: Characterization of wind and shear profiles from high-resolution radiosondes and ECMWF model, this proceedings.
- [7] Marseille, G.J., A. Stoffelen, 2003: Simulation of Wind Profiles from a space-borne Doppler Wind Lidar, Q.J.R. Meteorol. Soc., **129**, pp. 3079-3098
- [8] D. Tan, Andersson, E., M. Fisher, L. Isaksen, 2007: Observing-system impact assessment using a data assimilation ensemble technique: application to the ADM Aeolus wind profiling mission, Q.J.R. Meteorol. Soc., **133**, pp. 381-390